B meson spectrum and decay constant from $N_f = 2$ simulations

ALPHA
Collaboration

Benoît Blossier[* a]**, John Bulava**[b]**, Michele Della Morte** [c]**, Michael Donnellan** [b]**,
Patrick Fritzsch** [d]**, Nicolas Garron**[† e]**, Jochen Heitger** [f]**, Georg von Hippel** [c]**,
Björn Leder** [g]**, Hubert Simma** [b]**, Rainer Sommer** [b]

[a] *Laboratoire de Physique Théorique, CNRS et Université Paris-Sud XI, Bâtiment 210,
91405 Orsay Cedex, France*
[b] *NIC, DESY, Platanenallee 6, 15738 Zeuthen, Germany*
[c] *Universität Mainz, Institut für Kernphysik, Becherweg 45, 55099 Mainz, Germany*
[d] *School of Physics and Astronomy, University of Southampton, Southampton, SO17 1BJ, U.K.*
[e] *School of Physics and Astronomy, University of Edinburgh, Edinburgh EH9 3JZ, U.K.*
[f] *Universität Münster, Institut für Theoretische Physik, Wilhelm-Klemm-Strasse 9, 48149
Münster, Germany*
[g] *Universität Wuppertal, Gaussstr. 20, 42119 Wuppertal, Germany*

We report on the status of an ALPHA Collaboration project to extract quantities for *B* physics phenomenology from $N_f = 2$ lattice simulations. The framework is Heavy Quark Effective Theory (HQET) expanded up to the first order of the inverse *b*-quark mass. The couplings of the effective theory are determined by imposing matching conditions of observables computed in HQET with their counterpart computed in QCD. That program, based on $N_f = 2$ simulations in a small physical volume with Schrödinger functional boundary conditions, is now almost finished. On the other side the analysis of configurations selected from the CLS ensembles, in order to measure HQET hadronic matrix elements, has just started recently so that only results obtained at a single lattice spacing, $a = 0.07$ fm, will be discussed. We give our first results for the *b*-quark mass and for the *B* meson decay constant.

The XXVIII International Symposium on Lattice Field Theory, Lattice2010
June 14-19, 2010
Villasimius, Italy

---

[*]Speaker.
[†]Speaker.

1. Introduction

Now that the amount of available experimental data on beauty physics coming from the *B* factories and the Tevatron is large, and even more data are expected from the LHC, precision tests of the Standard Model and searches for New Physics have become possible in this area of flavor physics. Unfortunately, the theoretical uncertainty, mainly because of the difficult to estimate long-distance effects due to confinement, is currently limiting the impact of future experimental measurements on New Physics models. Lattice QCD makes it possible to reach a few percents of theoretical error on those non-perturbative hadronic contributions, but care is needed to obtain reliable results for *b*-quark physics. Indeed one has to keep under control simultaneously the finite size effects and, particularly, the discretisation effects (the lattice spacing should be smaller than the Compton wavelength of the *b*-quark) induced by the simulation. In practice it is not possible to control both effects in one simulation. Different approaches have been proposed in the literature (see for example [1] for a recent review). The ALPHA Collaboration has followed a strategy discussed in detail in [2] - [4]: it is based on the use of HQET, in which the hard degrees of freedom $\sim m_{\mathrm{b}}$ are integrated out and taken into account by an expansion in the inverse *b*-quark mass m_{b} . As discussed in those papers and also in earlier work, the benefit is the suppression of large discretisation effects which may arise in hadronic quantities when the theory is regularised on the lattice. The difficult aspect of that method is that a matching with QCD, which is the field theory believed to describe the strong interactions, is needed to absorb ultraviolet divergences appearing in the effective theory. In HQET those come as inverse powers of the lattice spacing and thus have to be removed non-perturbatively before the continuum limit can be taken. This method has been tested in the quenched approximation to study the B_{s} meson spectrum [5] and to determine the *b*-quark mass [3], the decay constant $f_{B_{\mathrm{s}}}$ [6], and the coupling $g_{\mathrm{B}^*\mathrm{B}\pi}$ [7].

The strategy, sketched in Fig. 1, is now being extended to the more realistic $N_{\mathrm{f}} = 2$ situation. In the next section, more details are given about the determination of HQET couplings, performed in a small physical volume (of space extent ~ 0.5 fm). In section 3, we report on the analysis of a subset of ensembles generated within the CLS effort, to get HQET energies and matrix elements. Section 4 contains our conclusions.

2. Computation of the relevant HQET parameters

We write the HQET Lagrangian as

$$\mathscr{L}_{\mathrm{HQET}}(x) = \mathscr{L}_{\mathrm{stat}}(x) - \omega_{\mathrm{kin}}\mathscr{O}_{\mathrm{kin}}(x) - \omega_{\mathrm{spin}}\mathscr{O}_{\mathrm{spin}}(x)\,, \tag{2.1}$$

where the lowest order (static) term is

$$\mathscr{L}_{\mathrm{stat}}(x) = \overline{\psi}_{\mathrm{h}}(x)\,D_0\,\psi_{\mathrm{h}}(x)\,, \tag{2.2}$$

and the first order corrections in $1/m_{\mathrm{b}}$ are

$$\mathscr{O}_{\mathrm{kin}}(x) = \overline{\psi}_{\mathrm{h}}(x)\mathbf{D}^2\psi_{\mathrm{h}}(x)\,, \quad \mathscr{O}_{\mathrm{spin}}(x) = \overline{\psi}_{\mathrm{h}}(x)\sigma\cdot\mathbf{B}\psi_{\mathrm{h}}(x)\,. \tag{2.3}$$

We are also interested in the time component of the heavy-light axial current A_0. Considering only the terms which contribute to zero-momentum correlation functions, we write it as

$$A_0^{\text{HQET}}(x) = Z_A^{\text{HQET}}[A_0^{\text{stat}}(x) + c_A^{(1)} A_0^{(1)}(x)], \tag{2.4}$$

$$A_0^{(1)}(x) = \overline{\psi}_1(x)\frac{1}{2}\gamma_5\gamma_i(\nabla_i^{\text{S}} - \overleftarrow{\nabla}_i^{\text{S}})\psi_{\text{h}}(x), \quad A_0^{\text{stat}}(x) = \overline{\psi}_1(x)\gamma_0\gamma_5\psi_{\text{h}}(x), \tag{2.5}$$

where ∇_i^{S} denotes the symmetric derivative.

In this section we present the computation of $\omega_{\text{kin}}, \omega_{\text{spin}}, Z_A^{\text{HQET}}, c_A^{(1)}$ and m_{bare} (the energy shift which in the static theory absorbs the $1/a$ divergence of the static energy and at order $1/m_b$ absorbs a $1/a^2$ term). These parameters can be used for a computation of the b-quark mass, the heavy-light meson decay constants (f_B or f_{B_s}), as well as for a determination of the spectrum of heavy-light mesons, including the hyperfine mass splitting. We follow the strategy presented in [4], where the computation was done in the quenched approximation. We recall here the essential ingredients and refer the reader to this paper for any unexplained notation and for more detailed explanations. This computation is done non-perturbatively (in the strong coupling), and at the $1/m_b$ order of the heavy quark expansion. The light quarks are simulated with 2-flavor Clover-improved Wilson fermions, and for the discretisation of the heavy quark we use the so-called HYP1 and HYP2 actions [8]. More details about the implementation can be found in [9]. The simulations considered in this section use the Schrödinger functional setup.

Following [4], we define a set of observables $\Phi_{i=1,\dots,5}$ that we collect in a vector Φ. In the continuum and large volume limits, Φ_1 is proportional to the meson mass and Φ_2 to the logarithm of the decay constant, respectively. Φ_3 is used to determine the counter-term of the axial current, and $\Phi_{4,5}$ for the determination of the kinetic and magnetic term, respectively. We first consider
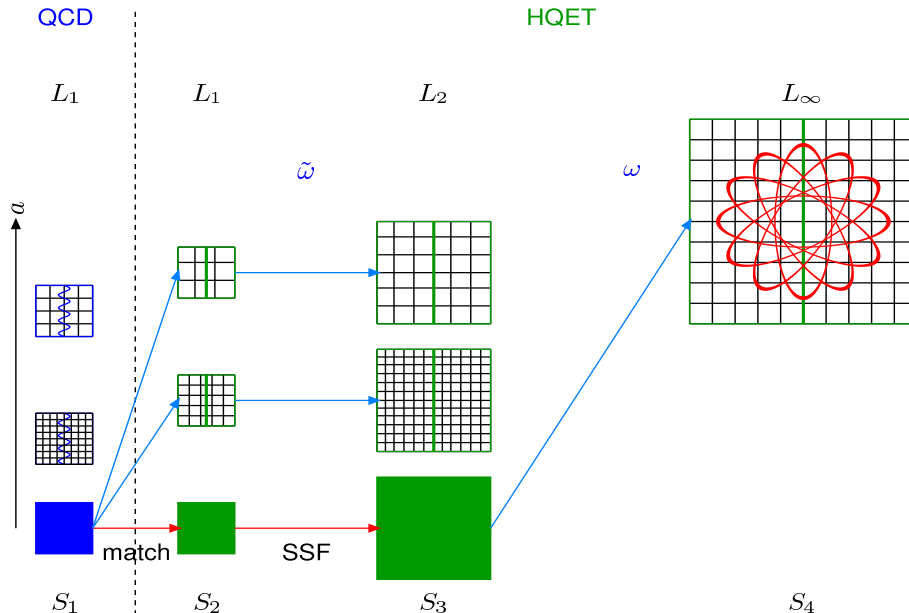
Figure 1: Sketch of the strategy followed by the ALPHA Collaboration to compute B physics observables on the lattice.

a small volume (of linear space extent $L_1 \sim 0.5$ fm), where the *b*-quark mass can be simulated with discretisation effects under control. In this volume, we compute the five observables Φ_i in QCD, for four different lattice spacings. In this set of simulations, the light quark masses are set to 0, while for the (RGI) heavy quark mass M we have chosen nine different values such that $z = L_1 M = 4, 6, 7, 9, 11, 13, 15, 18, 21$. The lightest masses correspond approximately to the charm and the heaviest to the bottom quark. In this work we will focus on the heaviest ones. The continuum limit of each observable is obtained by a linear extrapolation in $(a/L_1)^2$ of the three finest lattice spacings (except for the two heaviest masses where only the two finest lattices are used): $\Phi_i^{QCD}(L_1, M, 0) = \lim_{a \to 0} \Phi_i^{QCD}(L_1, M, a)$. This set of simulations is represented by S_1 in Fig. 1. The continuum extrapolations of the first two observables are shown in Fig. 2.
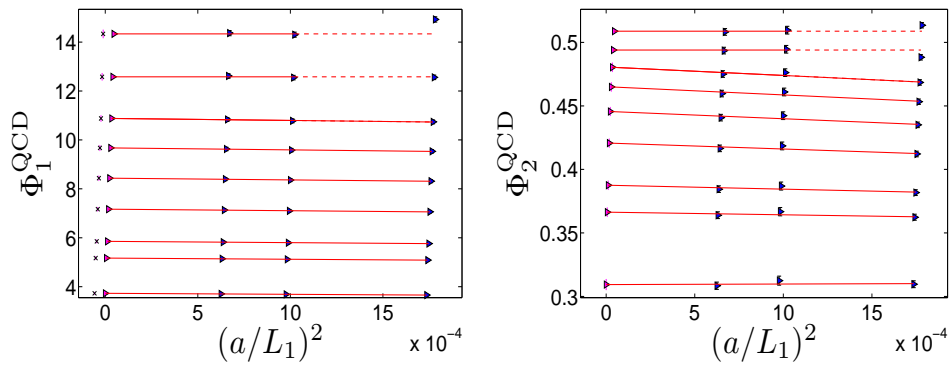
Figure 2: Continuum extrapolation of the QCD observables Φ_1 and Φ_2, which are proportional to the finite volume meson mass and to the finite volume logarithm of the decay constant, respectively. For Φ_1 we have included an error in the continuum coming from the renormalisation of the quark mass (cross on the left). Results are shown for the nine different values of the heavy quark mass.

In another set of simulations called S_2, we compute the corresponding quantities in the effective theory, using the same value of the physical volume. We then impose the QCD observables to be equal to their HQET expansion at the $1/m_b$ order [1]. This matching can be written in the following way:

$$\Phi_i^{QCD}(L_1, M, 0) = \eta_i(L_1, a) + \sum_j \varphi_{ij}(L_1, a)\, \tilde{\omega}_j(M, a) , \tag{2.6}$$

where η and φ are computed by lattice simulations for different values of the lattice spacing a. In other words the matching equations determine the set of parameters $\tilde{\omega} = \varphi^{-1}[\Phi^{QCD} - \eta]$. For example, in the the static approximation φ is diagonal and (up to a factor L_1) η_1 is given by the static energy, φ_{11} is one and $\tilde{\omega}_1$ is the bare quark mass in static approximation. In table 1, we list the various parameters together with their values in the static approximation and in the classical limit.

We then compute η and φ in a larger volume of space extent $L_2 = 2L_1$ using the same set of lattice spacings as the one used in the previous step. This step is represented by the set S_3. The observables in this volume are obtained from the parameters $\tilde{\omega}(M, a)$ determined in the previous

---

[1]Terms of order $1/m_b^2$ are dropped without notice.

ω_i	definition	classical value	static value
ω_1	m_{bare}	m_{b}	$m_{\text{bare}}^{\text{stat}}$
ω_2	$\log(Z_A^{\text{HQET}})$	0	$\log(Z_A^{\text{stat}})$
ω_3	$c_A^{(1)}$	$-1/(2m_{\text{b}})$	ac_A^{stat}
ω_4	ω_{kin}	$1/(2m_{\text{b}})$	0
ω_5	ω_{spin}	$1/(2m_{\text{b}})$	0

Table 1: Notation for HQET parameters, their values in classical and static approximation. For the numerical value of c_A^{stat}, we use the formula given in [10] .

step:

$$\Phi(L_2, M, 0) = \lim_{a \to 0} \left(\eta(L_2, a) + \varphi(L_2, a) \tilde{\omega}(M, a) \right) . \tag{2.7}$$

The continuum limit can be taken because the divergences cancel out in the previous equation. This procedure can then be re-iterated until the volume reached is large enough for finite size effects to be negligible, typically around $(2\,\text{fm})^3$. In practice, it turns out that three different volumes are enough (L_1, L_2 and the large volume one). Thus, the HQET parameters that can be used in large volume simulations (denoted as S_4) are given by

$$\omega(M, a) = \varphi^{-1}(L_2, a) \left[\Phi(L_2, M, 0) - \eta(L_2, a) \right] . \tag{2.8}$$

Finally we perform a small interpolation in β in order to obtain the parameters at the lattice spacing used in the CLS ensembles.

In general the equations (2.6) and (2.7) are meant to be taken at the $1/m_{\text{b}}$ order of HQET, but they are of course valid in the static approximation if one sets the various pieces to their static values. In that case, the observables will be denoted by Φ^{stat}, and otherwise we write Φ^{HQET}. We also define the $1/m_{\text{b}}$ correction to be $\Phi^{(1/m)} = \Phi^{\text{HQET}} - \Phi^{\text{stat}}$. As an illustration, we show some continuum extrapolations in the volume L_2: the first two observables in the static approximation in Fig. 3, and the $1/m_{\text{b}}$ corrections $\Phi_4^{(1/m)}$ and $\Phi_5^{(1/m)}$ (which are sensitive to the kinetic and magnetic parameter ω_{kin} and ω_{spin}) in Fig. 4. Note that the $1/m_{\text{b}}$ terms are extrapolated linearly in the lattice spacing, whereas in the static case the continuum extrapolation is done quadratically in the lattice spacing. This is justified because we use an $O(a)$-improved action and an $O(a)$-improved static axial current. We end this section by collecting in Table 2 the values of the HQET parameters used in the numerical applications reported in the following.

3. Extraction of HQET hadronic matrix elements

For the computation of the large-volume hadronic matrix elements, we ought to take the continuum limit and extrapolate in the up/down quark mass to the physical point where m_π has its physical value. The continuum extrapolation will be left for future work, we here just take a quite small lattice spacing, $a = 0.07\,\text{fm}$. We note that in our quenched computations the difference
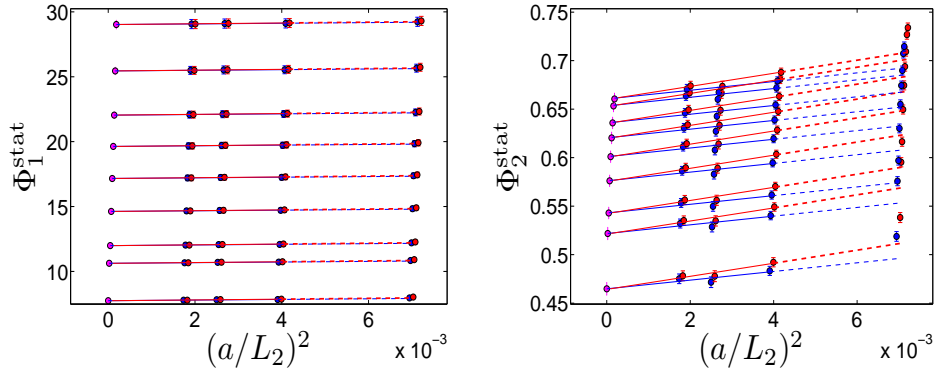
Figure 3: Continuum extrapolation of the static approximation of Φ_1 and Φ_2 in the volume of space extent L_2. The two different colors correspond to two different discretisations of the static propagator : red for HYP1 and blue for HYP2. Only the three finest lattice have been used in the continuum extrapolation.
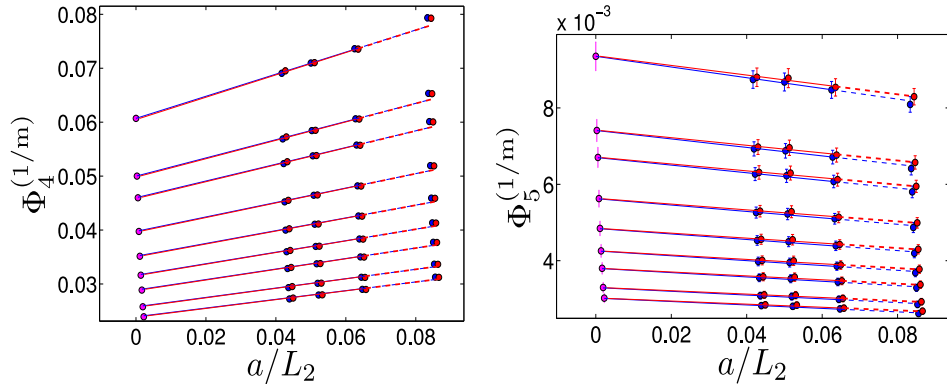
Figure 4: Same as Fig. 3 but for the $1/m_b$ terms $\Phi_4^{(1/m)}$ and $\Phi_5^{(1/m)}$, which are chosen to be proportional to ω_{kin} and ω_{spin}, respectively.

between the continuum limit and $a = 0.07\,\mathrm{fm}$ would be unnoticeable given the present errors. Concerning the extrapolation in the light quark mass, we take into account terms at NLO in the chiral expansion for the static approximation, but neglect terms of order m_{light}/m_b.

At the first order of the $1/m_b$ expansion our main observables are given by

$$m_{\mathrm{B}} = m_{\mathrm{bare}} + E^{\mathrm{stat}} + \omega_{\mathrm{kin}} E^{\mathrm{kin}} + \omega_{\mathrm{spin}} E^{\mathrm{spin}}, \tag{3.1}$$

$$m_{\mathrm{B}} - m_{\mathrm{B}^*} = \frac{4}{3} \omega_{\mathrm{spin}} E^{\mathrm{spin}}, \tag{3.2}$$

$$\log(a^{3/2} f_{\mathrm{B}} \sqrt{m_{\mathrm{B}}/2}) = \log(Z_{\mathrm{A}}^{\mathrm{HQET}}) + \log(a^{3/2} p^{\mathrm{stat}}) + b_{\mathrm{A}}^{\mathrm{stat}} a m_{\mathrm{q}}$$
$$+ \omega_{\mathrm{kin}} p^{\mathrm{kin}} + \omega_{\mathrm{spin}} p^{\mathrm{spin}} + c_{\mathrm{A}}^{(1)} p^{\mathrm{A}^{(1)}}, \tag{3.3}$$

where $b_{\mathrm{A}}^{\mathrm{stat}}$ is an improvement coefficient (in practice we follow [10] for its numerical implementation). The HQET energies and matrix elements have been measured on a subset of configuration ensembles produced within the CLS effort [11] with $N_f = 2$ flavors of $O(a)$-improved Wilson-Clover fermions. We have collected in Table 3 the main characteristics of that subset.

β	LM_Q	am_{bare}	$\log(Z_A^{\mathrm{HQET}})$	$[\log(Z_A)]^{(1/\mathrm{m})}$	$c_A^{(1)}/a$	ω_{kin}/a	ω_{spin}/a
5.3	15	41.125(22)	$-0.120(28)$	0.039(26)	$-0.446(75)$	0.476(06)	0.837(35)

Table 2: HQET parameters determined with the standard set of matching conditions, that are used to obtain the central values of m_{b} and f_{B}; the static quark action is HYP2 .

3.1 Large volume techniques

As interpolating fields we use quark bilinears

$$O_k(x) = \overline{\psi}_{\mathrm{h}}(x)\gamma_0\gamma_5\psi_1^{(k)}(x), \quad O_k^*(x) = \overline{\psi}_1^{(k)}(x)\gamma_0\gamma_5\psi_{\mathrm{h}}(x), \tag{3.4}$$

built from the static quark field $\psi_{\mathrm{h}}(x)$ and different levels of Gaussian smearing [12] for the light quark field

$$\psi_1^{(k)}(x) = \left(1 + \kappa_{\mathrm{G}}a^2\Delta\right)^{R_k}\psi_1(x), \tag{3.5}$$

with APE smeared links [13, 14] in the lattice Laplacian Δ, and with the same parameters as in [5]. We compute the following correlators

$$C_{ij}^{\mathrm{stat}}(t) = \sum_{x,\mathbf{y}}\left\langle O_i(x_0+t,\mathbf{y})O_j^*(x)\right\rangle_{\mathrm{stat}}, \tag{3.6}$$

$$C_{ij}^{\mathrm{kin/spin}}(t) = \sum_{x,\mathbf{y},z}\left\langle O_i(x_0+t,\mathbf{y})O_j^*(x)O_{\mathrm{kin/spin}}(z)\right\rangle_{\mathrm{stat}}, \tag{3.7}$$

$$C_{A^{(1)},i}^{\mathrm{stat}}(t) = \sum_{x,\mathbf{y}}\left\langle A_0^{(1)}(x_0+t,\mathbf{y})O_i^*(x)\right\rangle_{\mathrm{stat}}, \tag{3.8}$$

using stochastic all-to-all propagators to reduce the variance. From the $N \times N$ matrices of correlators C^{stat}, $C^{\mathrm{kin/spin}}$, and $C_{A^{(1)}}^{\mathrm{stat}}$, we solve the generalised eigenvalue problem (GEVP)

$$C(t)v_n(t,t_0) = \lambda_n(t,t_0)C(t_0)v_n(t,t_0), \tag{3.9}$$

to get the energies and operators having the largest overlap with the nth state:

$$aE_n^{\mathrm{eff}}(t,t_0) = -\ln\left(\frac{\lambda_n(t+a,t_0)}{\lambda_n(t,t_0)}\right), \tag{3.10}$$

$$Q_n^{\mathrm{eff}}(t,t_0) = \frac{O^i(t)v_n^i(t,t_0)}{\sqrt{v_n^i(t,t_0)C_{ij}(t)v_n^j(t,t_0)}}\left(\frac{\lambda_n(t_0+a,t_0)}{\lambda_n(t_0+2a,t_0)}\right)^{t/2a}. \tag{3.11}$$

β	a (fm)	$L^3 \times T$	m_π (MeV)	#	traj. sep.
5.3	0.07	$32^3 \times 64$	550	152	32
		$32^3 \times 64$	400	600	32
		$48^3 \times 96$	300	192	16
		$48^3 \times 96$	250	350	16

Table 3: Characteristics of the large volume simulations used so far to extract HQET energies and matrix elements. The last column is meant in terms of trajectories of length $\tau = 1$.

7

For a computation of the $1/m_b$ corrections to static energies and matrix elements one needs to solve the GEVP at the static order only [15]. For instance, in the case of energies, one has

$$E_n^{\text{eff}}(t,t_0) = E_n^{\text{eff,stat}}(t,t_0) + \omega E_n^{\text{eff},1/m}(t,t_0) + O(\omega^2) \, , \tag{3.12}$$

$$aE_n^{\text{eff,stat}}(t,t_0) = -\ln\left(\frac{\lambda_n^{\text{stat}}(t+a,t_0)}{\lambda_n^{\text{stat}}(t,t_0)}\right) \, , \tag{3.13}$$

$$E_n^{\text{eff},1/m}(t,t_0) = \frac{\lambda_n^{1/m}(t,t_0)}{\lambda_n^{\text{stat}}(t,t_0)} - \frac{\lambda_n^{1/m}(t+a,t_0)}{\lambda_n^{\text{stat}}(t+a,t_0)} \, , \tag{3.14}$$

$$\frac{\lambda_n^{1/m}(t,t_0)}{\lambda_n^{\text{stat}}(t,t_0)} = \sum_{i,j} v_{ni}^{\text{stat}}(t,t_0) \left[\frac{C_{ij}^{1/m}(t)}{\lambda_n^{\text{stat}}(t,t_0)} - C_{ij}^{1/m}(t_0) \right] v_{nj}^{\text{stat}}(t,t_0) \, . \tag{3.15}$$

As illustrated in the left panel of Fig. 5, a comparison with quenched data indicates that the statistical error on static energies is not an issue, even at small quark masses. Some care has to be taken to control the contribution of excited states to extracted energies. For the energy levels determined from the GEVP, the leading corrections are given by

$$E_n^{\text{eff,stat}}(t,t_0) = E_n^{\text{stat}} + \beta_n^{\text{stat}} e^{-\Delta E_{N+1,n}t} + \dots \tag{3.16}$$

where $\Delta E_{m,n} = E_m - E_n$ and the condition $t_0 \geq t/2$ is necessary to prove eq. (3.16). In our analysis we have chosen a time range to extract the plateaux such that the corrections to E_1^{stat} are small compared to its statistical error; we found this to be the case for $t_0 > 0.3$ fm.

3.2 b-quark mass

Once the energies are obtained at the simulated dynamical quark masses, we still need to extrapolate them to the physical point. We have chosen pion masses below 450 MeV for the
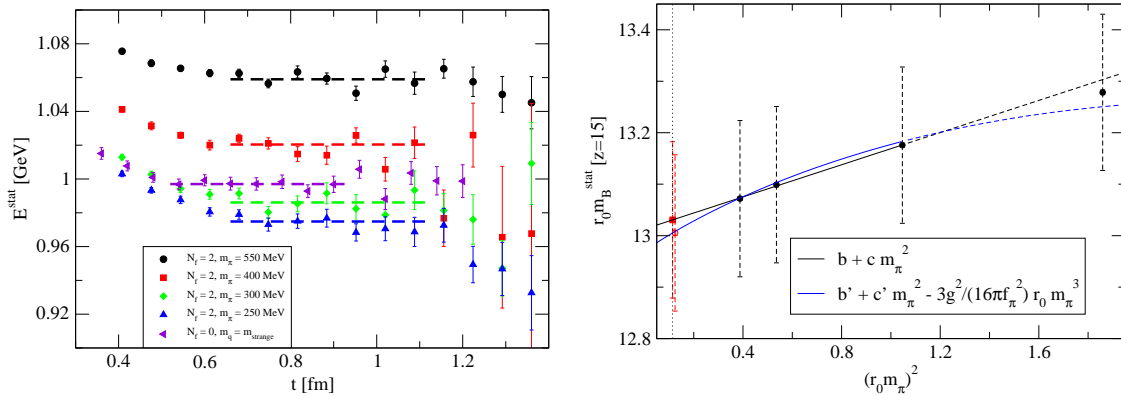
Figure 5: Plateaux of static energies with N=5 and $t_0 = 5a$ (left panel); the quenched data correspond to a lattice spacing quite close to the CLS set up at $\beta = 5.3$. We remind the reader that the absolute value of E^{stat} has no real meaning without the subtraction of a linear $1/a$ divergence. Right panel: chiral extrapolation of $r_0 m_B^{\text{stat}} = r_0(E^{\text{stat}} + m_{\text{bare}})$. A large part of the errors (dashed part), originating from r_0 and m_{bare}, is common to all data points and therefore irrelevant for the quark mass dependence.
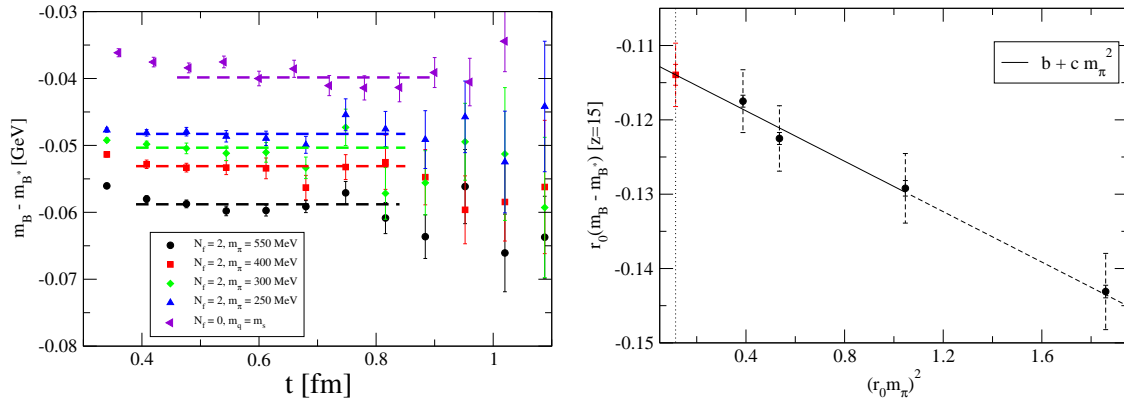
Figure 6: On the left panel we show the plateaux of $\omega_{\text{spin}}E^{\text{spin}}$ with $N=5$ and $t_0 = 4a$; the quenched data correspond to a lattice spacing quite close to the CLS set up at $\beta = 5.3$. On the right panel we show the chiral extrapolation of $r_0(m_{\text{B}} - m_{\text{B}^*})$ with a LO fit. Here the dashed error due to ω_{spin} and r_0 is independent of the quark mass.

extrapolation of all quantities reported in these proceedings. For the extrapolation of $m_{\text{B}}^{\text{stat}} \equiv E^{\text{stat}} + m_{\text{bare}}^{\text{stat}}$ we have used the following form

$$r_0 m_{\text{B}}^{\text{stat}} = b + c m_\pi^2 + d m_\pi^3, \tag{3.17}$$

where we once set $d = 0$, and once use $d = -3r_0\hat{g}^2/(16\pi f_\pi^2)$ computed with the experimental value of f_π and the recent lattice determination of $\hat{g} = 0.51(2)$ [7]. We show these fits in the right panel of Fig. 5. As our central value of $r_0 m_{\text{B}}^{\text{stat}}$ at the physical point we take the average of the two extrapolations. Half the difference is included in the systematic errors. At present a much larger source of uncertainty is r_0/a, whose determination is discussed in [17]. Moreover, an uncertainty of 5% has been added on the scale r_0 itself. We take $r_0 = 0.475 \pm 0.025$ fm [20–22]. Identifying the static approximation result, $m_{\text{B}}^{\text{stat}}$, with $m_{\text{B}}^{\text{exp}}$, we can determine the RGI b-quark mass from static HQET. Translating as usual to the $\overline{\text{MS}}$ scheme with 4-loop perturbation theory and the known Λ-parameter [18], we find

$$m_{\text{b}}^{\overline{\text{MS}}}(m_{\text{b}}^{\overline{\text{MS}}})_{\text{N}_f=2}^{\text{stat}} = 4.255(25)_{r_0}(50)_{\text{stat+renorm}}(?)_a \text{ GeV}, \tag{3.18}$$

where the first error comes from the uncertainty on r_0, while the second error includes the statistical error on aE^{stat}, the uncertainty on the chiral extrapolation and the error on the quark mass renormalisation constant Z_M in QCD [19]. The latter is currently dominating. The "$(?)_a$" indicates that a continuum limit is not yet performed, but as mentioned earlier we expect only a smaller error due to that [4].

Amongst the $O(1/m_{\text{b}})$ corrections to energies the hyperfine mass splitting is particularly interesting since here the $1/m_{\text{b}}$ term is the dominant one and is given by a single HQET parameter, ω_{spin}. This contribution can hence be discussed separately. Its determination is encouraging, as far as the statistical uncertainty and the chiral extrapolation are concerned, as shown in Fig. 6. Plateaux have the same quality as in the quenched case and the statistical precision is good enough to perform a reasonable chiral extrapolation. Since we have seen in the quenched approximation

that cut-off effects can be sizable for this quantity, we do not quote the hyperfine splitting in MeV at the moment.

Including the magnetic as well as the kinetic correction, we compute $m_B^{HQET} \equiv m_B^{stat+1/m}$, perform the chiral extrapolation as for m_B^{stat}, and from equating $m_B^{HQET} = m_B^{exp}$ we obtain the b-quark mass up to tiny Λ^3/m_b^2 effects as

$$m_b^{\overline{MS}}(m_b^{\overline{MS}})\Big|_{N_f=2}^{HQET} = 4.276(25)_{r_0}(50)_{stat+renorm}(?)_a \text{ GeV}. \tag{3.19}$$

Sources of errors are the same as in the static case. Some previous determinations read

$$m_b^{\overline{MS}}(m_b^{\overline{MS}})\Big|_{N_f=0}^{HQET} = 4.320(40)_{r_0}(48) \text{ GeV} \quad [3],$$
$$m_b^{\overline{MS}}(m_b^{\overline{MS}}) = 4.163(16) \text{ GeV} \quad [23].$$

In the future, a nice check of our result will consist in doing the same computation in a partially quenched set up; there, the experimental inputs will be the B_s spectrum, and the determination of the hopping parameter of the strange quark κ_s will be necessary. We will then be able to directly observe possible quenching effects because in the comparison with [3] we can use exactly the same experimental input. While the agreement with [23] is not convincing at the moment, it does not seem worrying given the present errors. We emphasize that within about 100 MeV all these numbers agree, while a more precise statement needs additional work, in particular the continuum limit on our side, and on a longer term $N_f > 2$.

3.3 B meson decay constant and V_{ub}

Let us now discuss f_B. In HQET we consider the particular combination [2]

$$\Phi_1 \equiv f_B \sqrt{m_B/2}, \tag{3.20}$$

see eq. (3.3). We separate the static and the $1/m_b$ contributions as

$$\log(r_0^{3/2}\Phi_1) = \log(r_0^{3/2}\Phi_1^{stat}) + [\log(\Phi_1)]^{(1/m)}, \tag{3.21}$$
$$[\log(\Phi_1)]^{(1/m)} = [\log(Z_A)]^{(1/m)} + \omega_{kin}p^{kin} + \omega_{spin}p^{spin} + (c_A^{(1)} - ac_A^{stat})p^{A^{(1)}}. \tag{3.22}$$

On the left panel of Fig. 7 we show that the GEVP method works as well as in the quenched case to extract the static matrix element. A good plateau is visible and our confidence in it is also based on the knowledge that corrections are $O(e^{-\Delta E_{N+1,n}t_0})$ when the computation is done as here (see [6, 15]). We have again applied two kinds of extrapolations of the static approximation $r_0^{3/2}\Phi_1^{stat}$ to the physical point [24]:

$$r_0^{3/2}\Phi_1^{stat} = b + cm_\pi^2 \quad (\text{LO}), \tag{3.23}$$
$$r_0^{3/2}\Phi_1^{stat} = b'\left[1 - \frac{3}{4}\frac{1+3\hat{g}^2}{(4\pi f_\pi)^2}m_\pi^2\ln(m_\pi^2) + c'm_\pi^2\right] \quad (\text{HM}\chi\text{PT}). \tag{3.24}$$

---

[2]We warn the reader that in this section we follow the notations introduced in [6], where the subscript 1 represents the ground state. In particular Φ_1 should not be confused with the finite volume meson mass Φ_1 introduced in section 2.
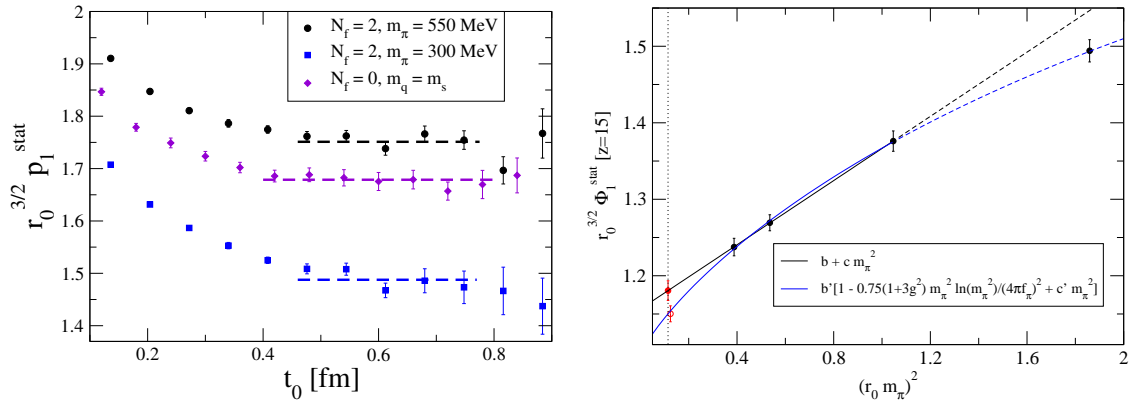
Figure 7: On the left panel we show the plateaux of $r_0^{3/2} p_1^{\text{stat}}$ with N=3 and $t - t_0 \sim 0.3$ fm; the quenched data correspond to a lattice spacing quite close to the CLS setup at $\beta = 5.3$. On the right panel we show the chiral extrapolation of $r_0^{3/2}\Phi_1^{\text{stat}}$.

Again we fixed $\hat{g}$ [7]. The same fit form is used for $r_0^{3/2}\Phi_1^{\text{HQET}}$. As shown in the right panels of Fig. 7 and Fig. 8, whether we do or do not include the chiral logarithm of HMχPT, changes the value at the physical point by a small but noticeable amount. At the moment we take the average of the two extrapolations as the central value and include half of the difference as part of the systematic error. We obtain

$$f_{\text{B}\ N_f=2}^{\text{HQET}} = 178(16)(?)_a\,\text{MeV}, \tag{3.25}$$

where the first error includes the statistical uncertainty on matrix elements, the systematics coming from chiral extrapolation and the uncertainty on the physical scale of r_0, while cut-off effects are not estimated yet. Let us recall that in the quenched approximation we have obtained $f_{\text{B}_s\ N_f=0}^{\text{HQET}} = 234(18)$ MeV [26] for $r_0 = 0.475$ fm and the error covers for a 5% uncertainty on r_0.

At present there is a tension between the two ways of determining V_{ub} from the exclusive B-decays $B \to \pi l \nu$ and $B \to \tau \nu$ [27]. Both of them rely on the determination of the hadronic matrix
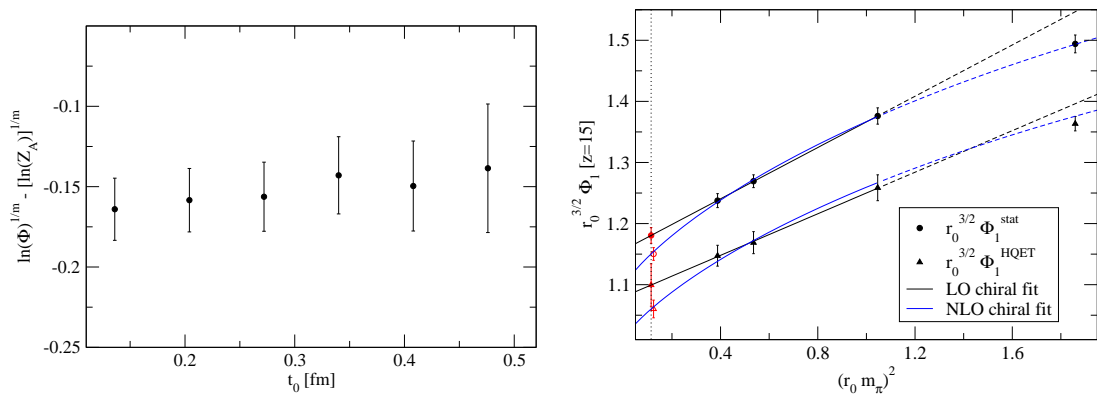
Figure 8: Plateau of $\log(\Phi_1)^{(1/m)} - [\log(Z_A)]^{(1/m)}$ for N=4, $t - t_0 = 4a$, $z = 15$ and $m_\pi \simeq 550$ MeV (left panel) and chiral extrapolation at the static order and at order $1/m$ (right panel).

Group	Method	Renormalisation	Range in a
ALPHA	HQET at $O(1/m_{\mathrm{b}})$	non-perturbative	$0.07\,\mathrm{fm}$
ETMC	twisted mass extrapolation in m_{b}	non-perturbative	$[0.065 - 0.1]\,\mathrm{fm}$
HPQCD	NRQCD	1-loop PT	$[0.09 - 0.12]\,\mathrm{fm}$
FNAL/MILC	Fermilab action	1-loop PT[3]	$[0.09 - 0.12]\,\mathrm{fm}$

Table 4: Present methods in lattice computations of f_{B} in unquenched simulations.

elements from lattice QCD. In the Standard Model, the branching ratio for the latter decay is simply proportional to $f_{\mathrm{B}}^2|V_{\mathrm{ub}}|^2$ with all other factors known. In Fig. 9, we have collected the values of f_{B} obtained recently by several collaborations [25], from $\mathrm{N_f} = 2$ (ALPHA, ETMC) and $\mathrm{N_f} = 2 + 1$ (FNAL/MILC, HPQCD) simulations. The heavy quark is discretised differently in each of the quoted computations: NRQCD (HPQCD), Fermilab action (FNAL/MILC), Twisted-Mass QCD (ETMC) and HQET (ALPHA). The systematic errors and difficulties in these different approaches are therefore rather different. For NRQCD a continuum limit does not exist and one studies a range of lattice spacings in the window between sizable discretisation errors and the divergent behaviour. In the relativistic twisted-mass approach one extrapolates in the heavy quark mass by assuming a HQET inspired form, and a continuum extrapolation has been performed. Some computations rely on perturbatively determined parameters. The FNAL/MILC and HPQCD computations use 1-loop renormalization[3] for the currents and part of the parameters in the Lagrangian. In our approach, all renormalization is done non-perturbatively and the theory has a continuum limit, but so far only a single lattice spacing of $a = 0.07$ fm is available in large volume. There is an intrinsic truncation error of $O(\Lambda^2/m^2)$ which is present (more or less explicitly) in all approaches.[4] We have sketched in Table 4 some of these issues. Despite the rather different characteristics, the results are very similar. The range of f_{B} in Fig. 9 does not reach large enough values to remove the tension between $B \to \tau\nu$ and $B \to \pi l\nu$ branching ratios within the Standard Model, and from Fig. 9 it seems very unlikely that the lattice determinations of f_{B} are the reason for the tension. However, interpreting this as a hint for physics beyond the Standard Model, one has to keep in mind that the $B \to \pi l\nu$ form factors are less well studied than f_{B} and that the experimental determination of the branching ratio $B \to \tau\nu$ is rather difficult.

4. Conclusions

We have reported on the status of the project undertaken by the ALPHA Collaboration to extract relevant B physics quantities from $\mathrm{N_f} = 2$ lattice simulations in the framework of HQET expanded at $O(1/m_{\mathrm{b}})$. The non-perturbative matching of HQET with QCD, through simulations performed in a small volume $L_1 \sim 0.5$ fm, is almost done. The measurement of HQET energies and matrix elements, using the GEVP approach, has started recently on ensembles produced by CLS. The analysis of quantities like the b-quark mass and the B decay constant is on the way. The first

---

[3]FNAL/MILC splits the renormalization factor into a non-perturbatively computed part and a rest estimated by 1-loop perturbation theory.

[4]Generically the truncation error is $\Lambda^2/m_{\mathrm{b}}^2$, but for the extrapolation in m significantly smaller masses enter.
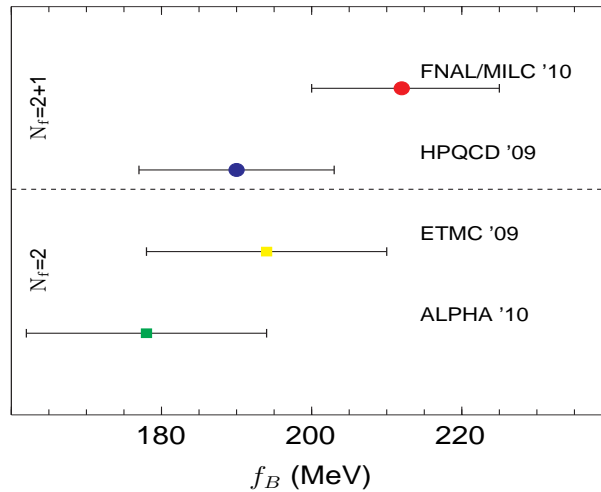
Figure 9: Collection of recent lattice computations of f_B.

results are promising and once we have controlled cut-off effects by simulation at several lattice spacings, we will also determine hadronic parameters of the $B - \bar{B}$ mixing or $B \to \pi$ semileptonic form factors as well as more details of the spectrum of hadrons with a b-flavor.

Acknowledgments

References

[1] J. Heitger, to appear in PoS LAT2010.

[2] J. Heitger and R. Sommer [ALPHA Collaboration], JHEP **0402**, 022 (2004) [arXiv:hep-lat/0310035].

[3] M. Della Morte, N. Garron, M. Papinutto and R. Sommer [ALPHA Collaboration], JHEP **0701**, 007 (2007) [arXiv:hep-ph/0609294].

[4] B. Blossier, M. Della Morte, N. Garron and R. Sommer [ALPHA Collaboration], JHEP **1006**, 002 (2010) [arXiv:1001.4783 [hep-lat]].

[5] B. Blossier, M. Della Morte, N. Garron, G. von Hippel, T. Mendes, H. Simma and R. Sommer [ALPHA Collaboration], JHEP **1005**, 074 (2010) [arXiv:1004.2661 [hep-lat]].

[6] B. Blossier, M. Della Morte, N. Garron, G. von Hippel, T. Mendes, H. Simma and R. Sommer [ALPHA Collaboration], [arXiv:1006.5816 [hep-lat]].

13

[7] J. Bulava, M. A. Donnellan and R. Sommer, PoS (Lattice 2010) 303 [arXiv:1011.4393 [hep-lat]].

[8] M. Della Morte, A. Shindler, and R. Sommer [ALPHA Collaboration], JHEP **051**, 08 (2005), [hep-lat/0506008]

[9] M. Della Morte, P. Fritzsch, J. Heitger, H. Meyer, H. Simma, and R. Sommer [ALPHA Collaboration], PoS LAT2007, **246** [hep-lat/0710.1188]

[10] A. Grimbach, D Guazzini, F. Knechtli and F. Palombi, JHEP **03**, [hep-lat/0802.0862]

[11] Coordinated Lattice Simulations, *https://twiki/cern.ch/twiki/bin/view/CLS/WebHome*.

[12] S. Güsken, U. Löw, K.-H. Mütter, R. Sommer, A. Patel and K. Schilling, Phys. Lett.**B227** (1989) 266.

[13] M. Albanese *et al.*, [APE Collaboration], Phys. Lett. B **192**,163 (1987).

[14] A. Lichtl, S. Basak, R. Edwards, G. T. Fleming, U. M. Heller, C. Morningstar, D. Richards, I. Sato, and S. Wallace, PoS LAT2005 **076** [hep-lat/0509179].

[15] B. Blossier, M. Della Morte, G. von Hippel, T. Mendes and R. Sommer [ALPHA Collaboration], JHEP **0904**, 094 (2009) [arXiv:0902.1265 [hep-lat]].

[16] J. L. Goity, Phys. Rev. D **46**, 3929 (1992) [arXiv:hep-ph/9206230].

[17] B. Leder *et al* [ALPHA Collaboration], to appear in PoS LAT2010.

[18] M. Della Morte *et al.* [ALPHA Collaboration], Nucl. Phys. **B713** (2005) 378-406. [hep-lat/0411025].

[19] P. Fritzsch, J. Heitger, N. Tantalo, JHEP **1008** (2010) 074. [arXiv:1004.3978 [hep-lat]].

[20] R. Baron *et al*, [ETM Collaboration], JHEP 1008:097,(2010) [arXiv:0911.5061 [hep-lat]]

[21] C. T. H. Davies *et al.* [HPQCD Collaboration], Phys. Rev. **D81** (2010) 034506. [arXiv:0910.1229 [hep-lat]].

[22] Y. Aoki, S. Borsanyi, S. Dürr *et al.*, JHEP **0906** (2009) 088. [arXiv:0903.4155 [hep-lat]].

[23] K. G. Chetyrkin, J. H. Kühn, A. Maier, P. Maierhofer, P. Marquard, M. Steinhauser and C. Sturm, Phys. Rev. D **80**, 074010 (2009) [arXiv:0907.2110 [hep-ph]].

[24] S. R. Sharpe and Y. Zhang, Phys. Rev. D **53**, 5125 (1996) [arXiv:hep-lat/9510037].

[25] E. Gamiz, C. T. H. Davies, G. P. Lepage, J. Shigemitsu and M. Wingate [HPQCD Collaboration], Phys. Rev. D **80**, 014503 (2009) [arXiv:0902.1815 [hep-lat]];
B. Blossier *et al.* [ETM Collaboration], JHEP **1004**, 049 (2010) [arXiv:0909.3187 [hep-lat]];
J. Simone *et al* [FNAL/MILC], to appear in PoS LATT2010.

[26] B. Blossier *et al.* [ALPHA Collaboration], arXiv:1006.5816 [hep-lat].

[27] F. Porter, talk given at ICHEP 2010.

14